J. Membrane Biol. 129, 189–198 (1992)

The Journal of
Membrane Biology

Involvement of Different S_4 Parts in the Voltage Dependency of Na Channel Gating

Zipora Kra-Oz†‡, Gad Spira‡, Yoram Palti†, and Hamutal Meiri†

† Department of Physiology and Biophysics and ‡Laboratory of Cell Biology, The Bruce Rappaport Faculty of Medicine and The Rappaport Family Institute for Research in The Medical Sciences, Technion-Israel Institute of Technology, Haifa 31096, Israel

Summary. Three synthetic peptides corresponding to parts of S_4 of the first repeat of eel electroplax sodium channel were synthesized. The basic peptide was C_I^+ which corresponds to amino acids 210–223 (eel channel numbering) and two subfractions: an external fraction, $C_{I\,ex}^+$ (amino acid 210–217); and an internal part, $C_{I\,in}^+$ (amino acid 218–221). Peptide C_I^+ includes four of the charged amino acids of this domain; peptide $C_{I\,ex}^+$ includes three of the charged amino acids and is closer to the external membrane surface (according to channel models) than peptide $C_{I\,in}^+$ which includes the fourth charged amino acid alone.

Antibodies generated in rabbits against these peptides were shown to be site specific. Using the whole-cell patch-clamp technique, we found that in rat dorsal root ganglion (DRG) cells, the antibodies against $C_{I\,in}^+$ but not against $C_{I\,ex}^+$ had an effect on the gating parameters. They shifted the Na-channel inactivation curve towards hyperpolarization and decreased the slope of the Na-channel activation curve. These results demonstrate that during the conformational changes associated with channel gating, the fourth charged amino acid of S_4 must be accessible to antibodies given to the external solution. Furthermore, they indicate a specific involvement of S_4 in the voltage dependency of the gating processes.

Key Words whole cell patch clamp · synthetic peptides · dorsal root ganglion · eel electroplax · antibodies

Introduction

Voltage-sensitive sodium channels are responsible for the initial rapid increase in membrane permeability to sodium ions, which is essential for the generation of most action potentials (Hodgkin & Huxley, 1952; Armstrong, 1981; Hille, 1984). Analysis of the primary structure of sodium channels revealed four repeats (Noda et al., 1984), each containing 6–8 transmembrane segments S_1-S_n (Noda et al., 1984, 1986; Greenblatt, Blatt & Montal, 1985; Guy & Seetharamulu, 1987; Kosower, 1985).

Among the transmembrane segments, the S_4 has a unique structure: a series of positively charged amino acids (arg^+ and lys^+) with two nonpolar amino acids intervening between them (Noda et al., 1984, 1986). This structure is typical to all voltage-gated cation channels (Tanabe et al., 1987; Papazian et al., 1988). The orientation of the S_4 in the membrane as suggested by Noda et al. (1986) was supported by Stühmer et al. (1989) for Na channels and for potassium channels by Papazian et al. (1991). The results of studies utilizing antibodies against S_4 are also consistent with this view (Sammar, Spira & Meiri, 1992).

Most models of the sodium channels propose that the S_4 participates in sensing the membrane field or potential during the gating process (Noda et al., 1984, 1986; Greenblatt et al., 1985; Guy & Seetharamulu, 1986; Kosower, 1985; Catterall, 1988). This involvement received experimental support by the work of Stühmer et al. (1989) who have shown that replacement of one, two or three charged amino acids of S_4 with neutral ones decreased the slope of Na-channel conductance *vs.* membrane potential curve. They also found that the decrease in the slope is proportional to the number of charged amino acids replaced in S_4. From experiments utilizing anti-S_4 antibodies it was independently deduced that S_4 is also associated with Na-channel inactivation (Meiri et al., 1987; Meiri, Sammar & Schwartz, 1989; Schwartz, Palti & Meiri, 1990).

Gating is attributed in all models to conformational changes in the channel molecule in response to depolarization. These changes may result in the exposure to the external solution of channel domains, which are embedded in the membrane at the resting state. For example, the "sliding helix model" (Catterall, 1988) proposes that at resting potential the S_4 forms a helix in the membrane so that all its positively charged amino acids are embedded in the membrane and are neutralized by negatively charged amino acids. According to this model, the S_4 helix slides out upon depolarization, effectively transposing one or two of the positively charged amino acids of the S_4 towards the external membrane surface.

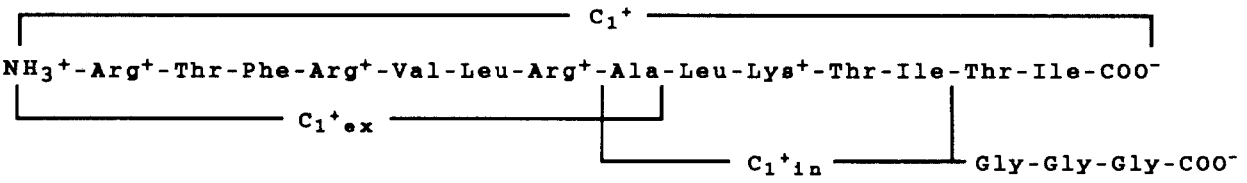

Fig. 1. Peptide sequence. A scheme that presents the sequences of peptide C_1^+, which corresponds to a part of S_4 of the first internal repeat of eel electroplax Na channel, and peptides $C_{1\,ex}^+$ and $C_{1\,in}^+$ derived from it. A three-glycine tail was added to peptide $C_{1\,in}^+$.

The "propagating helix model" (Guy & Conti, 1990) and the "helical screw mechanism" (Guy & Durell, 1991) suggest that upon depolarization a significant part of S_4 moves outward and becomes exposed on the outer membrane surface. During this process at least three and perhaps four charged amino acids of S_4 are exposed to the external medium. The experimental results of Pusch (1990) indicate that this region becomes accessible to the extracellular solution upon depolarization, thus supporting this model.

In an attempt to clarify the changes in the sodium-channel molecule associated with gating, the exposure of S_4 to the external solution during this process was studied.

Antibodies were raised against synthetic peptides corresponding to two intramembrane parts of S_4: $C_{1\,ex}^+$, situated close to the external surface, and $C_{1\,in}^+$ which is buried deeper in the membrane. The experiments were designed to address the following questions: (i) Are the two parts of the S_4 accessible to antibodies given to the external solution? (ii) How is channel function modified by antibodies against these subfractions of S_4? The results are interpreted with reference to the different channel-gating models.

Materials and Methods

Peptide Structure

C_1^+ is a synthetic peptide corresponding to the S_4 of repeat *I* of the eel electroplax sodium channel (amino acids 210–223). It includes four charged amino acids. The peptide was previously used to generate anti-S_4 antibodies which were employed to study S_4 orientation in the membrane (Sammar et al., 1992). They were also shown to modify Na-channel inactivation (Meiri et al., 1987, 1989; Schwartz et al., 1990). Here we used two subfractions of C_1^+: the part assumed to be close to the external surface of the membrane (according to models) denoted $C_{1\,ex}^+$ (amino acids 210–217, eel channel numbering). This part contains three of the four charged amino acids of C_1^+. The part assumed to be deeper in the bilayer, denoted $C_{1\,in}^+$ (amino acids 218–221), includes only the fourth charged amino acid and had an additional three-glycine tail (Fig. 1).

Two other peptides were used as controls: (i) S_4IV, a synthetic peptide corresponding to the S_4 segment of the fourth internal repeat of the Na channel (Tosteson, Auld & Tosteson, 1989). (This peptide was made available to us by courtesy of Dr. M. Tosteson, Harvard Medical School, Boston, MA.) (ii) The peptide "dipole" corresponding to a region near the N terminus of the sodium channel, amino acids 1690–1699. This peptide consists of three positively charged amino acids and three negatively charged amino acids (Sammar et al., 1992).

Peptide Synthesis and Conjugation

Peptides were synthesized using the solid-phase technique (Merrifield, 1985) by Penninsula Laboratories Europe (St. Helens, UK), and their compositions were verified by amino acid analysis. The peptides were coupled to KLH (Calbiochem, San Diego, CA), or BSA (Sigma, St. Louis, MO) using EDCI (Sigma). The peptide-carrier conjugates were dialyzed against 0.1 M ammonium bicarbonate and stored at −20°C.

Immunization

Rabbits were immunized by multistage subcutaneous and intramuscular injections of KLH-peptide conjugate mixed with complete Freund's adjuvant, as detailed elsewhere (Sammar et al., 1992).

ELISA Procedure

Immunoplates were coated with 10–50 μg/ml of peptides or membranes, and ELISA was carried out as detailed elsewhere (Meiri et al., 1989). IgG content was measured using goat anti-rabbit IgG (Sigma) and standard Ig.

Crude Electroplax Membrane Fractions (EMF)

Electroplax membranes were prepared according to Miller, Agnew and Levinson (1983). A stored organ was thawed, sliced, homogenized in grinding buffer [50 mM potassium phosphate, 5 mM EDTA, and 0.1 mM PMSF, pH 6.8] and centrifuged. The supernatant was ultraspun at 100,000 × *g*. The pellet was resuspended in grinding buffer and stored in liquid nitrogen. All steps were conducted at 4°C.

Preparation of Crude Liver Membrane (CLM)

Rat liver was homogenized with mannitol buffer (0.3 M mannitol, and 1 mM EDTA, pH 7.4), centrifuged, and the supernatant was collected and recentrifuged. The pellet was collected into mannitol buffer and used or stored in liquid nitrogen. All processing steps were carried out at 4°C.

Preparation of Rat Brain Membrane (RBM)

Rat brain (Kanner, 1980) was homogenized in mannitol buffer, centrifuged, and the supernatant was recentrifuged. The pellet was loaded onto a ficoll step gradient, centrifuged and the synaptosomes were collected, washed with mannitol buffer, lysed with hypotonic buffer (5 mM EDTA, and 10 mM Tris-Cl, pH 7.4), centrifuged, and the pellet was stored in liquid nitrogen.

Membrane Solubilization

Membranes were mixed with solubilizing buffer (100 mM choline chloride, 10 mM EDTA, 10 mM EGTA, and 50 mM potassium phosphate, pH 7.4, and 5% Triton X-100 containing 100 mM PMSF, 1 mM iodoacetamide and 1 mM pepstatin), incubated at 4°C, and precipitated by centrifugation.

Saxitoxin (STX) Binding

Five to sixty nM ^{3}H-STX (New England Nuclear, Boston, MA, specific activity of 37.3 Ci/mmol at 1 mCi/ml) were mixed with channels or membrane samples, and incubated for 60 min at 4°C. The reaction was terminated by rapid filtration through Whatmann GF/C filters. Filters were counted by liquid scintillation counter. Specific binding was determined after subtraction of the binding in the presence of 1 μM tetrodotoxin (Duch & Levinson, 1987).

Immunoprecipitation and Phosphorylation of Sodium Channel

Solubilized EMF or RBM (1 pmol STX binding sites) were incubated for 16 hr at 4°C with 200 μg of antibodies (purified on protein-A column) and the antibody-antigen complexes were precipitated by protein-A-Sepharose. Immunoprecipitated samples were washed with phosphorylation buffer (5 mM $MgCl_2$, 5 mM EDTA, and 25 mM HEPES-Tris, pH 7.4, and 0.1–0.5% Triton X-100), and radiolabeled using the catalytic subunit of cAMP-dependent protein kinase (Sigma) and 10 μCi of γ-^{32}P-ATP (New England Nuclear) according to Schmidt et al. (1985). The reaction was terminated by ice-cold termination buffer (100 mM sodium phosphate, pH 7.4, 20 mM EDTA, 50 mM KF, and 0.5% Triton X-100), washed in RIA buffer (50 mM sodium phosphate, pH 7.4, 20 mM KF, 75 mM NaCl, 2.5 mM EDTA, 0.01% NaN_3, and 0.5% Triton X-100), and centrifuged. Labeled samples were electrophoresed on 4–15% polyacrylamide gradient SDS gel (Laemmli, 1970), and autoradiography was done on Kodak XM-5 papers.

Culturing of DRG Cells

Lumbar and sacral dorsal root ganglia (DRG) of 5–8-day-old rats were isolated and single cells were obtained as detailed before (Schwartz et al., 1990). Cells (10^3–10^4) were seeded on poly-L-lysine coated petri dishes with 1.5 ml medium and cultured for 4–10 hr at 37°C. Neurons (10–15 μm in diameter) were distinguished from Schwann cells by their round shape and bright halo.

Whole Cell Patch Clamp

Heat-polished, machine-pulled, hard-glass pipettes having a DC resistance of 3–5 $\times$ 10^6 Ω when filled with internal solution were used. The composition of extracellular solution was (in mM): 100 NaCl, 2 Na_2HPO_4, 5 KCl, 10 glucose, 5 HEPES, 40 TEA-Cl, and 2.5 $MgCl_2$. Intracellular solution consisted of (in mM): 10 NaCl, 130 CsCl, 2.5 $MgCl_2$, 5 HEPES, 5 EGTA, and 5 KCl. The pH of both solutions was adjusted to 7.35. Potassium and calcium currents were abolished as detailed by Schwartz et al. (1990).

The whole-cell patch-clamp technique (Hamill et al., 1981) was applied using a 10^9-Ω headstage (LIST, EPC-7). The procedures for minimizing capacitance and for corrections of the leakage current and the series resistance were described before (Schwartz et al., 1990).

A data general "desktop-30" computer with analog-to-digital and digital-to-analog converters was used to generate command potentials and to digitize membrane currents at sampling rates of 2–24 kHz at 10-bit resolution. The currents were low-pass filtered at 10 kHz. All experiments were performed at room temperature (25 $\pm$ 2°C). Only cells with pure fast or pure slow sodium currents were used for this study. These two current types were described by Schwartz et al. (1990).

Current-voltage curves were obtained using a 40-msec prepulse to -150 mV for the fast Na current or to -50 mV for the slow Na current. The prepulses were followed by 40-msec test pulses in the range from -70 to $+80$ mV at 5–10-mV increments. Holding potential was -70 mV, and pulse interval was 3 sec.

The maximal Na-current value [$I_{Na(peak)}$] at each membrane potential (V_m) was plotted against V_m to obtain the I-V curve. $I_{Na(max)}$ was defined as the largest $I_{Na(peak)}$ of the I-V curve. Sodium conductance, g_{Na}, was calculated from

$$g_{Na} = I_{Na}/(V_m - V_{Na}) \quad (1)$$

where V_{Na} was the experimentally measured current reversal potential. V_{Na} was very close to the Nernst equilibrium potential for sodium.

The relative conductance (m_∞) was calculated from the peak conductance $g_{Na(peak)}$ at each V_m normalized by the maximal conductance [$g_{Na(max)}$].

To obtain h_∞ curves two protocols were used. For the slow Na current we used 40-msec prepulses (V_{pp}) in the range of -70 to 0 mV which were followed by 5-msec long test pulses (V_t) to $V_m = +5$ mV. For the fast Na current V_{pp} ranged from -160 to -30 mV and V_t was to $V_m = +25$ mV. Inactivation was determined from the ratio between the $I_{Na(peak)}$ obtained following any V_{pp} and the largest I_{Na}.

Antibody Application

Extracellular application was achieved by adding the antibodies (purified on a protein-A column) to the perfusing solution at a concentration of 100 μg IgG/ml. When the effect was established,

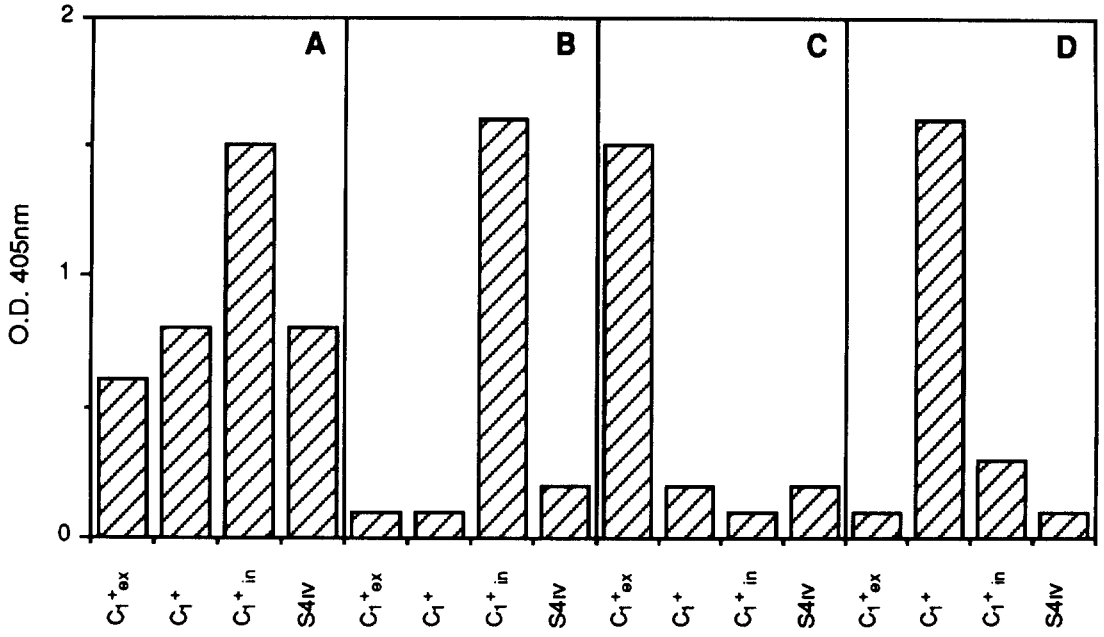

Fig. 2. Cross-reaction. Binding of antipeptide antibodies with the corresponding and related peptides. ELISA plates were coated with 10 μg of a peptide. The antibodies were diluted to give 75% of the maximum binding of each antibody to its respective peptide and reacted with the other peptides. (*A*) Anti-$C_{I\,in}^{+}$ (serum 304), (*B*) anti-$C_{I\,in}^{+}$ (serum 301), (*C*) anti-$C_{I\,ex}^{+}$ (serum 303), and (*D*) anti-C_{I}^{+}. S_4IV, A peptide obtained from Tosteson et al. (1989) which corresponds to the S_4 of the fourth internal repeat.

it reached saturation within 15–20 min. Measurements were taken immediately after the patch was formed and at 5-min intervals after the addition of the antibodies.

Results

Immunochemical Interaction of Antibodies with the Peptides and with the Na Channel

In this study we found that the antisera generated in rabbits against the external part of C_I^+ (denoted $C_{I\,ex}^{+}$) and against its internal part ($C_{I\,in}^{+}$) recognized their corresponding peptides in ELISA assay (Fig. 2). The binding of anti-$C_{I\,ex}^{+}$ was specific to its respective peptide. This antibody did not cross-react with the other S_4 peptides (Fig. 2*C*). Among the antisera generated against $C_{I\,in}^{+}$ two types were identified; while the serum of rabbit 301 did not cross-react with the other peptides tested (Fig. 2*B*), the serum of rabbit 304 interacted with all other S_4 peptides tested (Fig. 2*A*). Anti-C_I^+ reacted only with C_I^+ (Fig. 2*D*). All antisera listed above, including anti-$C_{I\,in}^{+}$ of rabbit 304, did not cross-react with the peptide denoted dipole corresponding to a region near the C terminus of the Na channel (Sammar et al., 1992).

All the antibodies against subfractions of S_4 reacted in ELISA with excitable membranes isolated from eel electroplax and rat brain and not with membranes of rat liver (*not shown*).

Anti-$C_{I\,in}^{+}$ and anti-$C_{I\,ex}^{+}$ immunoprecipitated Na channels from solubilized preparation of eel electroplax and rat brain membranes. The immunoprecipitated channels were detected either by in-vitro phosphorylation (Schmidt, Rossie & Catterall, 1985) with cAMP-dependent protein kinase (Fig. 3*A*) or by ^{3}H-STX binding (Gordon et al., 1987). In the latter, the binding was increased in proportion to the amount of antibodies employed (Fig. 3*B*). These results coincide with a previous report by Sammar et al. (1992) who demonstrated the immunoprecipitation of Na channels by anti-C_I^+. All together these results emphasize the presence of specific anti-sodium channel antibodies in the antipeptides antisera.

Electrophysiological Effects

Steady-State Inactivation

The antibodies against $C_{I\,in}^{+}$ shifted the h_∞ curve of the fast adult (FA)-type Na current towards hyperpolarization by 18.6 ± 6 mV ($\bar{X}$ ± SD, n = 10, IgG of rabbit 304) and by 11.5 ± 1.7 mV (n = 7, IgG of rabbit 301, Table 1, *A*, Fig. 4*A* and *B*). Regardless of the differences between them, the effects of each of these antibodies was significantly larger than the

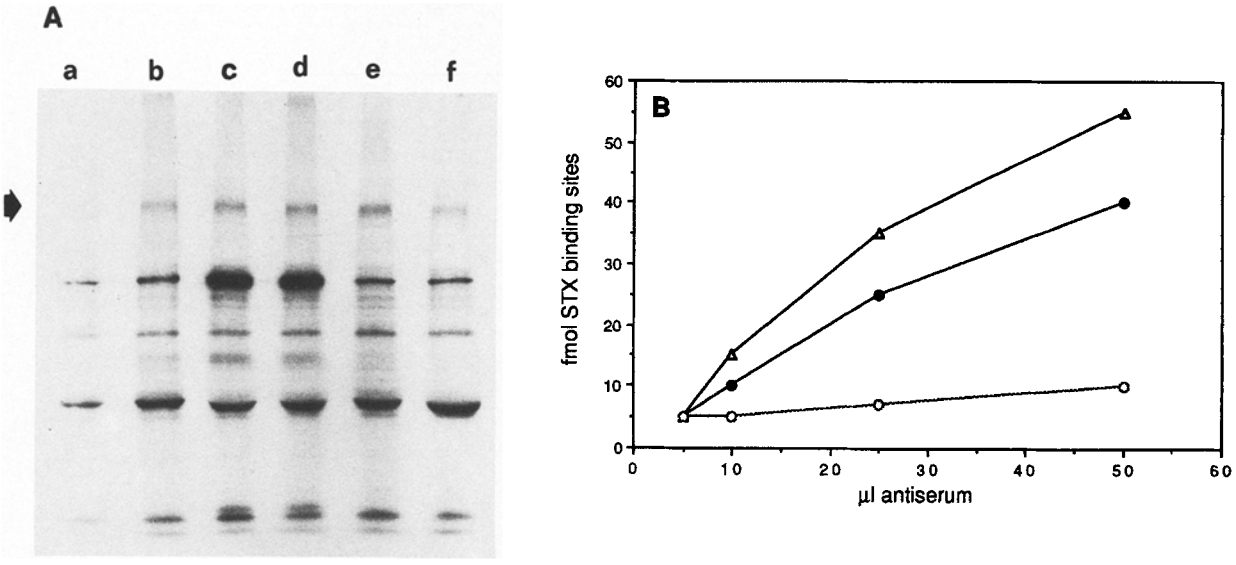

Fig. 3. Immunoprecipitation. (*A*) Na channels were immunoprecipitated from solubilized eel electroplax membranes followed by phosphorylation with cAMP-dependent protein kinase. Labeled bands are shown following 5–15% polyacrylamide gel electrophoresis and autoradiography. Arrowhead: a 270-kD band. *a*, Normal rabbit IgG; *b*, anti-C_I^+, *c and d*, anti-$C_{I\,in}^+$ (serum 304); *e*, anti-$C_{I\,in}^+$ (serum 301); and *f*, anti-$C_{I\,ex}^+$ (serum 303). (*B*) Na channels were immunoprecipitated from solubilized eel electroplax membranes using increasing amounts of antibodies. The amount of precipitated Na channels was measured using 10 nM ^{3}H-STX. Values are shown after subtraction of nonspecific binding obtained with 10 μM TTX. Open circles, normal rabbit IgG; filled circles, anti-$C_{I\,ex}^+$ (serum 303); and open triangles, anti-$C_{I\,in}^+$ (serum 304).

effect of normal rabbit IgG ($P < 0.01$, Table 1, *A*, Fig. 4*D*). These shifts were smaller than the shift of 25 ± 5.8 mV produced by anti-C_I^+ as reported by Schwartz et al. (1990). The antibodies against $C_{I\,in}^+$ did not change the slope of inactivation.

Anti-$C_{I\,ex}^+$ had no significant effect on the inactivation of the FA-type Na current (Fig. 4*C*, Table 1, *A*).

None of the antibodies had any effect on the inactivation of the slow Na current (Table 1, *B*).

Steady-State Activation

Anti-$C_{I\,in}^+$ decreased the slope of the steady-state activation curve (m_∞) of the FA-type current (Fig. 5*A* and *B*), whereas anti-$C_{I\,ex}^+$ and normal rabbit IgG had no effect (Fig. 5*C* and *D*). Note that Schwartz et al. (1990) found that the antibodies against C_I^+ have no effect on m_∞.

The voltage dependency of m_∞ can be described (Stühmer et al., 1989) by

$$m_\infty(V_m) = 1/\{1 + \exp[Z_m e_0(V - V_m^{1/2})/kT]\} \qquad (2)$$

where e_0 is the electron charge, k is the Boltzmann's constant, T is the absolute temperature, Z_m is the valence of the apparent single gate charge for activation, V_m is the membrane potential and $V_m^{1/2}$ is the value of V_m where $m_\infty = 0.5$.

From Eq. (2) it is seen that Z_m determines the slope of the m_∞ *vs.* voltage curve.

The values of Z_m for the fast Na current of DRG cells were in the range of 4.4–5.1 (Table 2). Calculation of Z_m values, on the basis of m_∞ curves given in other studies of DRG cells (Kostyuk, Veselovsky & Tsyndrenko, 1981; Orozco, Epstein & Rapoport, 1988), yielded similar values. These Z_m values are larger than those reported by Stühmer et al. (1989) for Na channels from rat brain. It is not an easy task to accurately determine small differences in the steepness of activation from m_∞ measurements. However, the analysis of the changes in the slope of m_∞ shows (Table 2, Fig. 5) that anti-$C_{I\,in}^+$ reduced significantly the slope of m_∞. The mean change of Z_m by anti-$C_{I\,in}^+$ (serum 304 and 301) was 1.27 ± 1.1 (Table 2). This effect on the slope was statistically larger ($P < 0.055$ two-tailed t test) than the effect produced by normal rabbit IgG, 0.15 ± 0.87. These results indicate that the antibodies against the internal part of the S_4 decrease the slope of the Na-channel activation curve.

None of these antibodies significantly shifted the m_∞ curve of Na conductance along the voltage axis (Table 1, *A*).

The activation of slow Na current was not affected by any of the antibodies (Table 1, *B*).

Table 1. Modification of slow and fast Na channels by antibodies
A. Fast adult (FA) Na current

Average changes		Antibodies against				Normal rabbit serum (n = 6)
		$C^+_{1\,in}$ 301 (n = 7)	$C^+_{1\,in}$ 304 (n = 10)	$C^+_{1\,ex}$ 303 (n = 8)	*C^+_1 (n = 6)	
Vh_{50}	(mV)	−11.5 ± 1.7[a]	−18.6 ± 6[a]	−4.5 ± 3	−25.0 ± 5.8[b]	−4.3 ± 1.4
Vg_{50}	(mV)	3.8 ± 3.4	−1.2 ± 5	−1.6 ± 6.1	3.1 ± 1.1	1.0 ± 4.5
V_{Na}	(mV)	−1.0 ± 4.2	−1.3 ± 6.4	4.9 ± 2.1	5.0 ± 0.8	5.1 ± 3.3
V-I_{max}	(mV)	0.7 ± 4.1	5.0 ± 4.7	−1.9 ± 3.5	NM[c]	−1.6 ± 0.5
I^{Ab}_{max}	(%)	68.0 ± 13	60.0 ± 8.3	60.0 ± 17	78.0 ± 17	55.0 ± 13

B. Slow (S) Na current

Average changes		Antibodies against				Normal rabbit serum (n = 4)
		$C^+_{1\,in}$ 301 (n = 3)	$C^+_{1\,in}$ 304 (n = 4)	$C^-_{1\,ex}$ 303 (n = 6)	C^+_1 (n = 9)	
Vh_{50}	(mV)	4.0 ± 3.5	−6.0 ± 5.8	−4.0 ± 3.7	−6.8 ± 4.7	−4.1 ± 1.7
Vg_{50}	(mV)	2.2 ± 1.3	2.6 ± 2.3	−3.6 ± 2.4	2.8 ± 2.5	−2.6 ± 1.7
V_{Na}	(mV)	5.6 ± 0.5	−2.6 ± 3.7	0.8 ± 4.6	5.4 ± 4.2	−1.3 ± 1.4
V-I_{max}	(mV)	5.5 ± 2.5	0.0 ± 3.1	0.9 ± 3.4	NM[c]	−3.4 ± 3.7
I^{Ab}_{max}	(%)	63.0 ± 12	62.0 ± 6.9	77.5 ± 12	67.0 ± 15.5	69.0 ± 4.5

A summary of the mean shifts ($\bar{X}$ ± SD) of electrophysiological parameters of: A, fast (FA)-type and B, slow (S)-type Na currents. The parameters were measured after 20-min application of antibodies (100 μg/ml) to the external solution. Vh_{50}, membrane potential at 50% inactivation; Vg_{50}, membrane potential at 50% activation; V_{Na}, reversal potential of Na current; V-I_{max}, membrane potential where maximal I_{Na} measured; and I^{Ab}_{max}, the relative size of $I_{Na(max)}$ (%) left in the presence of the antibodies. Statistical significance was evaluated with reference to the effect of normal rabbit serum (NRS). [a] $P <$ 0.001, [b] $P < 0.01$ for a two-tailed t test (antibody compared to NRS). * values of the effect of anti-C^+_1 taken from Schwartz et al. (1990). [c] Not measured.

Other Na-Current Parameters

As summarized in Table 1, none of the antibodies had any significant effect on the amplitude of maximal Na current (I_{max}), on the potential where this peak is obtained (V-I_{max}), and on the reversal potential (V_{Na}). The above findings suggest that the shift of h_∞ along the voltage axis is due to a local effect on inactivation and cannot be attributed to a general shift in the voltage-dependent parameters.

Discussion

The S_4 of many voltage-dependent cation channels has a positively charged amino acid at each third position. This unique arrangement is considered to have a role in the gating of cation channels (Noda et al., 1984, 1986; Greenblatt et al., 1985; Kosower, 1985; Guy & Seetharamulu, 1986; Catterall, 1988; Guy & Conti, 1990; Papazian et al., 1991). The experiments described here utilized site-specific antibodies against the external ($C^+_{1\,ex}$) and the internal ($C^+_{1\,in}$) parts of S_4 of sodium channels in order to address two questions: (i) Are both the external and the internal parts of S_4 accessible to antibodies applied at the external membrane surface? (ii) If and in what way is channel function modified following the application of such antibodies? The results of this work indicate that the region containing the fourth (counting from the outer side) charged amino acid is accessible to antibodies applied at the external surface and that antibodies against the latter region modify both activation and inactivation.

Antibody Specificity

The antibodies against $C^+_{1\,ex}$ and $C^+_{1\,in}$ were site specific excluding one antiserum that cross-reacted with the other subfractions of S_4 but not with peptides

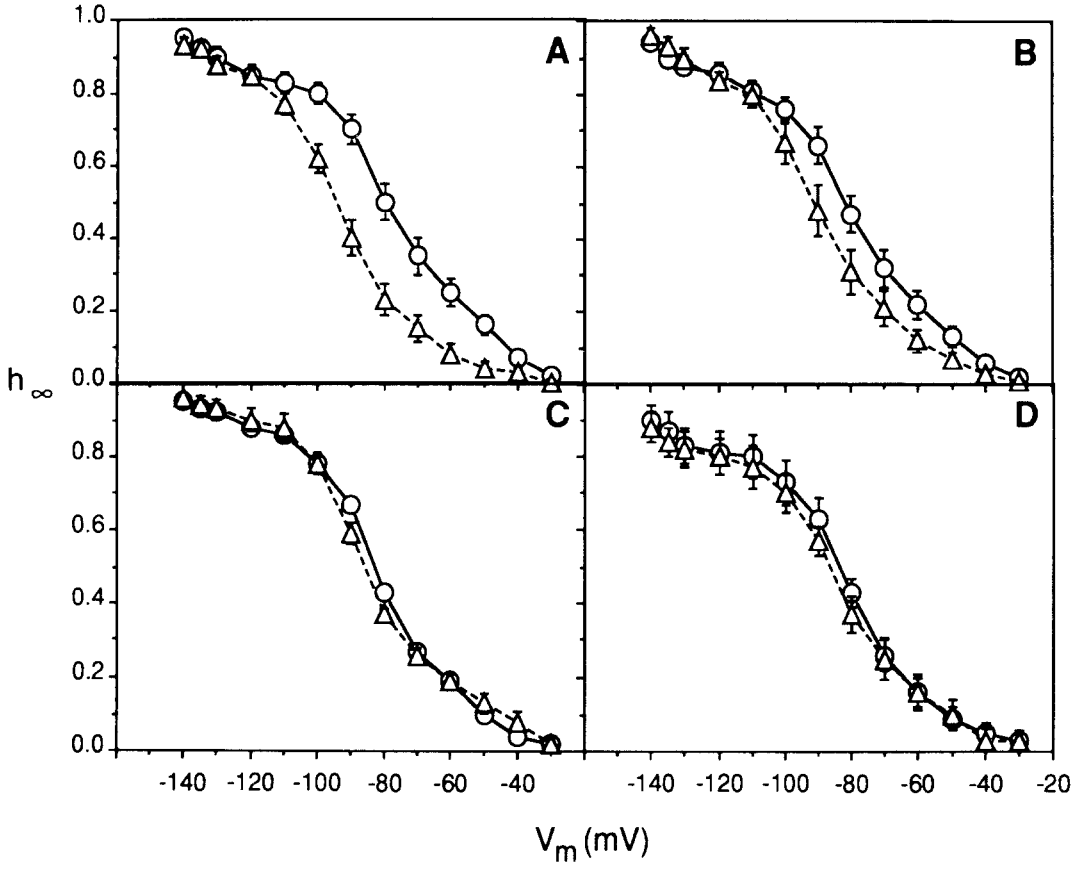

Fig. 4. Steady-state inactivation *vs.* membrane potential curves (h_∞). Circles, controls; triangles, following 20-min incubation with 100 μg/ml antibodies. Values are means ± SEM. (*A*) Anti-$C_{I\,in}^+$ (serum 304, 10 cells), (*B*) anti-$C_{I\,in}^+$ (serum 301, 7 cells), (*C*) anti-$C_{I\,ex}^+$ (serum 303, 8 cells), and (*D*) normal rabbit IgG (5 cells).

corresponding to a region outside S_4. The antibodies immunoprecipitated sodium channels from solubilized membranes of eel electroplax and rat brain synaptosomes, indicating that the antibodies recognize their corresponding epitopes on sodium channel molecules. Thus, the antibodies to subfractions of S_4 can be used as markers of their domains.

The possibility that the antibodies may bind to epitopes outside the examined segment was investigated by searching for all potential antigenic determinants composed of sequences of three amino acids (the smallest antigenic determinant) of the peptides. The analysis was applied to eel electroplax and rat brain Na channels (Noda et al., 1984, 1986). The analysis revealed that there are only two triplets homologous to $C_{I\,in}^+$ situated on S_4 in continuation with $C_{I\,in}^+$ deeper in the membrane. Three triplets homologous to $C_{I\,ex}^+$ were found on other S_4 segments, and a fourth homologous triplet (LRA) is located at the exteracellular loop between segment S_5 and S_6 of repeat *I*. These findings indicate that, in spite of the large size of the Na channel, with only one exception, the antigenic determinants for the antibodies to S_4 fragments are all localized on S_4s.

Analysis of Electrophysiological Effects

Steady-State Inactivation

Consistent with the negative shift of the inactivation curve by anti-C_I^+ (Schwartz et al., 1990), the antibodies to $C_{I\,in}^+$ were found to shift the curve toward hyperpolarization. The inactivation was the only voltage-dependent process of the Na channel that was shifted along the voltage axis. The shift can reflect a modification of the effective electric field experienced by the voltage sensor of the inactivation process, while the inactivation process itself (as reflected by the unchanged slope of the inactivation curve) is not modified. A negative shift of the voltage dependency of h_∞ may result from neutralization of

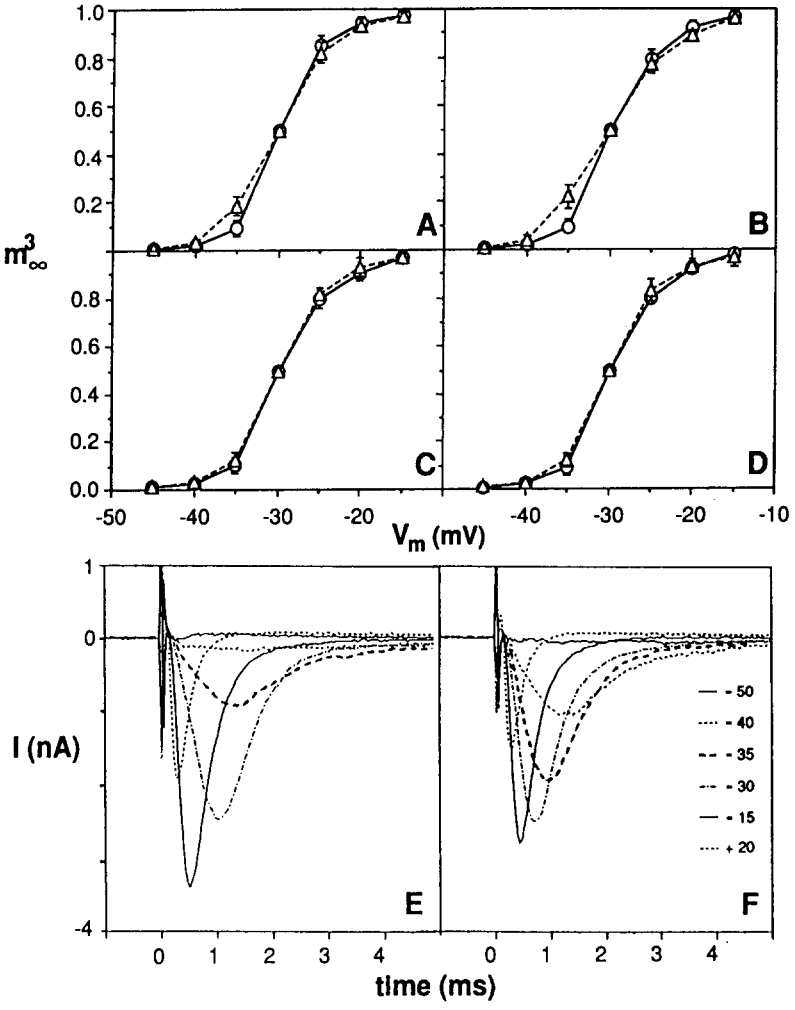

Fig. 5. Steady-state activation *vs.* membrane potential curves (m^3_∞). Circles, control; triangles, 20 min after addition of antibody to the external solution. Values are means ± SEM. (*A*) Anti-$C^+_{1\,in}$ (serum 301, 7 cells), (*B*) anti-$C^+_{1\,in}$ (serum 304, 10 cells), (*C*) anti-$C^+_{1\,ex}$, (serum 303, 6 cells), (*D*) normal rabbit IgG (5 cells), (*E*) control traces of sodium current (uncorrected for capacity transients), and (*F*) traces 20 min after application of anti-$C^-_{1\,in}$ (serum 304).

the positive charges on S_4, such as the fourth positive charge which corresponds to the one of $C^+_{1\,in}$. In the experiments of Stühmer et al. (1989) neutralization of this positive charge of S_4 did not result in a significant negative shift of the h_∞ curve. It is therefore possible that the antibodies have an effect beyond the neutralization *per se*.

Sammar et al. (1992) reported that the binding of anti-C^+_1 with rat brain synaptosomes increases with depolarization. This was interpreted as a higher affinity of the antibody to the inactive state. Based on this finding it can be assumed that the binding of anti-$C^+_{1\,in}$ is also state dependent with preference to the inactive state. If such binding locks the channel in the inactivated state it would lead to a shift of the inactivation curve to the left.

The results of this study do not necessarily mean that the "voltage sensor" of inactivation is on the region corresponding to $C^+_{1\,in}$ on S_4. It is possible that the antibodies to $C^+_{1\,in}$ bind to their site and thereby allosterically change a remotely located inactivation mechanism. As the above is true for anti-$C^+_{1\,in}$ of serum 301, which was entirely specific to its corresponding peptide, it can be concluded that the internal part of S_4 (the region which contains the fourth charged amino acid) is accessible to antibodies applied externally.

Steady-State Activation

The slope of the activation curve was decreased following the exposure to anti-$C^+_{1\,in}$. Anti-$C^+_{1\,ex}$ and normal rabbit IgG had no effect. A change in the slope of activation is usually considered to be an effect on the activation process itself (Armstrong, 1981). The decrease in the slope of activation by anti-$C^+_{1\,in}$ is consistent with the finding of Stühmer et al. (1989). From the slope of the curve we calculated that anti-$C^+_{1\,in}$ decreased Z_m, the mean decrease being approximately one. This can be interpreted as an indication that the antibodies effectively neutralize

Table 2. Changes of Z_m by the antibodies

Antibody	Z_m		No. of cells	Mean changes of Z_m
	Before Ab ($\bar{X} \pm$ SD)	With Ab ($\bar{X} \pm$ SD)		
Anti-$C^+_{I\,in}$ (301 + 304)	4.95 ± 1.15	3.67 ± 1.09	17	1.27 ± 1.1[a]
Anti-$C^+_{I\,ex}$ (303)	4.42 ± 0.78	4.41 ± 1.13	6	0.01 ± 0.99
Normal rabbit IgG	4.80 ± 0.56	4.65 ± 0.40	5	0.15 ± 0.87

The table summarizes the average values of Z_m of controls and those obtained 20 min after addition of 100 μg/ml antibodies to the external solution.
[a] $P < 0.055$ for two-tailed t test (antibody compared to NRS).

the single positively charged amino acid in $C^+_{I\,in}$. Alternatively the antibody binding may be assumed to lock the channel in the activated state following the outward movement of S_4. Such fixation would reduce the number of elements that move with depolarization and thus reduce the slope of the m_∞ curve.

From the above it may be concluded that anti-$C^+_{I\,in}$ may lock the channel in whatever state it finds it—the activated or the inactivated state. Locking the channel in either of these states would shift the h_∞ toward hyperpolarization.

It is interesting that anti-$C^+_{I\,in}$ affects both activation and inactivation. This is consistent with the review of Armstrong and Bezanilla (1977) who have suggested that activation and inactivation are coupled.

How Can We Understand the Lack of Effect of Anti-$C^+_{I\,EX}$ on Both Activation and Inactivation?

Several reasons could be given: (i) The antibodies *bind* to the $C^+_{I\,ex}$ region of the channel, but this region has no role in gating (i.e., only the inner part of C^+_I is associated with gating). This assumption is not consistent with the results of Stühmer et al. (1989). (ii) The antibodies *bind* to the $C^+_{I\,ex}$ region, which may have a role in channel gating, but the binding does not interfere with its function. (iii) Anti-$C^+_{I\,ex}$ fails to recognize its epitopes on DRG channels but interacts with homologous segments. (iv) Under our experimental conditions, anti-$C^+_{I\,ex}$ does not recognize its epitope on the Na channels.

Unfortunately, we cannot rule out any of the above.

Structure-Function Relationships

All channel models attribute gating, at least in part, to conformational changes in S_4. In some models S_4 is assumed to be embedded in the membrane at the resting potential and to become partially exposed to the external solution upon depolarization. The models differ, however, with respect to the details of the process and the degree of S_4 exposure to the external solution. The effects of anti-$C^+_{I\,in}$ on gating strongly suggest that the fourth charged amino acid of S_4 is accessible to antibodies applied from the external membrane surface, at least part of the time. Among available sodium-channel models, the "propagating helix model" of Guy and Conti (1990) and the "helical screw mechanism" of Guy and Durell (1991) propose that this part of S_4 is exposed to the external medium during channel gating. In other channel models, the proposed conformational changes are more restricted (Greenblatt et al., 1985; Kosower, 1985; Catterall, 1988), and channel structure is considered to be too rigid to allow the exposure of the fourth charged amino acid (Stühmer et al., 1989). Our results support models like that of Guy and Conti (1990) or Guy and Durell (1991) that assume a large movement of S_4s during gating.

We wish to express our gratitude to Dr. M. Tosteson (Harvard Medical School) for providing us with samples of peptide S_4IV to use in the ELISA assays. We thank Dr. R. Gordon (The Max Planck Institute for Biophysics, Frankfurt) for immunochemical advise and protocols. The advice of Drs. M. Sammar, M. Paizi, R. Schatzberger, I. Zeitoun and Y. Mika (Technion) was very useful. We thank Mrs. A. Schwartz (Technion) for participating in the experiments.

This study was supported by a basic research grant of The Israel Academy of Sciences and Humanities (#430.87 to H.M. and G.S.).

References

Armstrong, C.M. 1981. Sodium currents and gating currents. *Physiol. Rev.* **61**:644–683

Armstrong, C.M., Bezanilla, F. 1977. Inactivation of the sodium channel II. Gating current experiments. *J. Gen. Physiol.* **70**:567–590

Catterall, W.A. 1988. Structure and function of voltage sensitive ion channels. *Science* **242**:50–61

Duch, D.S., Levinson, S.R. 1987. Neurotoxin-modulated uptake of sodium by highly purified preparation of the electroplax tetrodotoxin-binding glycoprotein reconstituted into lipid vesicles. *J. Membrane Biol.* **98:**43–55

Gordon, R.D., Fieles, W.E., Schotland, D.L., Hogue-Angeletti, R., Barchi, R.L. 1987. Topographical localization of the C-terminal of the voltage-dependent sodium channel from *Electrophorus electricus* using antibodies raised against a synthetic peptide. *Proc. Natl. Acad. Sci. USA* **84:**308–312

Greenblatt, R.E., Blatt, Y., Montal, M. 1985. The structure of the voltage sensitive sodium channels. Inferences derived from computer-aided analysis of the *Electrophorus electricus* channel primary structure. *FEBS Lett.* **193:**125–134

Guy, H.R., Conti, F. 1990. Pursuing the structure and function of voltage-gated channels. *Trends Neurosci.* **13:**201–206

Guy, H.R., Durell, S. 1991. A detailed structural model of the transmembrane portion of voltage gated potassium channels. *Physiologist* **34:**6.8

Guy, H.R., Seetharamulu, P. 1986. Molecular model of the action potential sodium channel. *Proc. Natl. Acad. Sci. USA* **83:**508–512

Hamill, O.P., Marty, A., Neher, E., Sakmann, B., Sigworth, F. 1981. Improved patch-clamp technique for high resolution current recording from cells and cell-free membrane patches. *Pfluegers Arch.* **391:**85–100

Hille, B. 1984. Ionic Channels of Excitable Membrane. pp. 426. Sinauer, Sunderland (MA)

Hodgkin, A.L., Huxley, A.F. 1952. A quantitative description of membrane current and its application to conduction and excitation in nerve. *J. Physiol.* **116:**500–544

Kanner, B.I. 1980. Modulation of neurotransmitter transport by the activity of the action potential sodium ion in membrane vesicles from rat. *Biochemistry* **19:**692–697

Kosower, E.M. 1985. A structural and dynamic molecular model for the sodium channel of *Electrophorus electricus*. *FEBS Lett.* **182:**235–242

Kostyuk, P.G., Veselovsky, N.S., Tsyndrenko, A.Y. 1981. Ionic currents in the somatic membrane of rat dorsal root ganglion neurons. I. Sodium currents. *Neuroscience* **12:**2423–2430

Laemmli, U.K. 1970. Cleavage of structural proteins during the assembly of the head of bacteriophage T_4. *Nature* **227:**680–685

Meiri, H., Sammar, M., Schwartz, A. 1989. Production and use of synthetic peptide antibodies to map a region associated with sodium channel inactivation. *Methods Enzymol.* **178:**714–739

Meiri, H., Spira, G., Sammar, M., Namir, M., Schwartz, A., Komoriya, A., Kosower, E.M., Palti, Y. 1987. Mapping a region associated with Na channel inactivation using antibodies to a synthetic peptide corresponding to a part of the channel. *Proc. Natl. Acad. Sci. USA* **84:**5058–5062

Merrifield, R.B. 1985. Solid phase synthesis. *Angew. Chem. Int. Ed. Engl.* **24:**799–810

Miller, J.A., Agnew, W.S., Levinson, S.R. 1983. Principal glycopeptide of tetrodotoxin/saxitoxin binding protein from *Electrophorus electricus:* Isolation and partial physical characterization. *Biochemistry* **22:**461–470

Noda, M., Ikeda, T., Kayano, T., Suzuki, H., Takeshima, H., Kurasaki, M., Takahashi, H., Numa, S. 1986. Existence of distinct sodium channel messenger RNA in rat brain. *Nature* **320:**188–192

Noda, M., Shimizu, S., Tanabe, T., Takai, T., Kayano, T., Ikeda, T., Takahashi, H., Nakayama, H., Kanaoka, Y., Miniamino, N., Kangawa, K., Matsuo, H., Raftery, M.A., Hirose, T., Inayama, S., Hayashida, H., Miyata, T., Numa, S. 1984. Primary structure of *Electrophorus electricus* sodium channel deduced from cDNA sequence. *Nature* **312:**121–127

Orozco, C.B., Epstein, C.J., Rapoport, S.I. 1988. Voltage-activated sodium conductances in cultured normal and trisomy 16 dorsal root ganglion neurons from the fetal mouse. *Dev. Brain Res.* **38:**265–274

Papazian, D.M., Schwarz, T.L., Temple, B.L., Timpe L.C., Jan, L.Y. 1988. Ion channel in *Drosophila*. *Annu. Rev. Physiol.* **50:**379–394

Papazian, D.M., Timpe, L.C., Jan, Y.N., Jan, L.Y. 1991. Alteration of voltage dependence of *shaker* potassium channel by mutations in the S_4 sequence. *Nature* **349:**305–310

Pusch, M. 1990. Divalent cations as probes for structure-function relationships of cloned voltage-dependent sodium channels. *Eur. Biophys. J.* **18:**327–333

Sammar, M., Spira, G., Meiri, H. 1992. Depolarization exposes the voltage sensor of the sodium channels to the extracellular region. *J. Membrane Biol.* **125:**1–11

Schmidt, J.W., Rossie, S., Catterall, W.A. 1985. A large intracellular pool of inactive sodium channel α subunit in developing rat brain. *Proc. Natl. Acad. Sci. USA* **82:**4847–4851

Schwartz, A., Palti, Y., Meiri, H. 1990. Structural and development differences between three types of Na channels in dorsal root ganglion cells of newborn rats. *J. Membrane Biol.* **116:**117–128

Stühmer, W., Conti, F., Suzuki, H., Wang, X., Noda, M., Yahagi, N., Kubo, N., Numa, S. 1989. Structural parts involved in activation and inactivation of the sodium channel. *Nature* **339:**597–603

Tanabe, T., Takeshima, H., Mikami, A., Flockerzi, V., Takahashi, H., Kangawa, K., Kojima, M., Matsuo, H., Hinose, T., Numa, S. 1987. Primary structure of the receptor for calcium channel blockers from skeletal muscle. *Nature* **328:**313–318

Tosteson, M.T., Auld, D.S., Tosteson, D.C. 1989. Voltage gated channels formed in lipid bilayers by a positively charged segment of the Na-channel polypeptide. *Proc. Natl. Acad. Sci. USA* **86:**707–710

Received 23 October 1991; revised 12 February 1992